Vorticity Deposition, Structure Generation and the Approach to Self-Similarity in Colliding Blast Wave Experiments

A.P.L.Robinson[a], H.Schmitz[a], T.E.Fox[b,a], J.Pasley[b,a], D.R.Symes[a]

[a] *Central Laser Facility, STFC Rutherford-Appleton Laboratory, Didcot, Oxfordshire, OX11 0QX, United Kingdom*
[b] *York Plasma Institute, University of York, York, YO10 5DD, United Kingdom*

Abstract

When strong shocks interact with transverse density gradients, it is well known that vorticity deposition occurs. When two non-planar blast waves interact, a strong shock will propagate through the internal structure of each blast wave where the shock encounters such density gradients. There is therefore the potential for the resulting vorticity to produce pronounced density structures long after the passage of these shocks. If the two blast waves have evolved to the self-similar (Sedov) phase this is not a likely prospect, but for blast waves at a relatively early stage of their evolution this remains possible. We show, using 2D numerical simulations, that the interactions of two 'marginally young' blast waves can lead to strong vorticity deposition which leads to the generation of a strong protrusion and vortex ring as mass is driven into the internal structure of the weaker blast wave.

Keywords: blast wave, laser, vorticity

1. Introduction

The generation of vorticity and multi-scale structure in fluids subjected to multiple shocks is an important problem in a number of areas in astrophysics, high-energy density physics, and inertial fusion. It is important in the study of star formation as this is dependent on the development of fine structure in the interstellar gas [1, 2]. Certain theories [3, 4] aimed at accounting for the intergalactic magnetic field depend on a seed magnetic field that in turn arises from vorticity generated in shock interactions in the pre-galactic medium. Supernova remnants are blast-driven systems that are well-known for their complex structure and morphologies [5]. In both the astrophysical context of supernova ejecta and inertial fusion, shock-deposited vorticity can drive mixing [6] which is important to both areas of study [7].

The development of high-powered laser technology has allowed researchers to study energetic, compressible hydrodynamical systems, including blast waves [8]. Vorticity generation and magnetic field generation (via the Biermann battery effect) has been studied for laser-driven blast waves [9]. There are a range of different methods for launching blast waves in laser-driven experiments. Some of these allow for considerable control, e.g. cluster targets [10], which has greatly expanded the range of experimental possibilities. Experiments which might produce supersonic turbulence are currently being considered [11].

The flexibility of blast wave experiments based on cluster media has made it relatively easy to pursue studies of blast wave collisions [12, 10]. The production of multiple, interacting blast waves is, of course, possible with other laser-target configurations and other HEDP drivers. It is well known that the interaction of strong shocks with density inhomogeneities leads to copious vorticity deposition and thus the formation of corresponding density structures (e.g. shock-bubble interactions [13]). The implication of this is that studies of shock-deposition of vorticity could be pursued experimentally with systems in which two strong explosions interact.

In this paper we consider a hypothetical experiment in which two moderately asymmetric blast waves are launched and interact. This leads to a situation where shocks cross the interior region of each blast wave (which we refer to as the 'cavity'). The inhomogeneities in the density and sound speed of the unshocked material might be thought to lead to significant shock-deposition of vorticity which can then lead to complex density structure being produced. However there are also good reasons to doubt that significant vorticity can be generated, e.g. weak density gradients in the central region of a Sedov-Taylor solution. We suggest that if the blast waves are relatively 'young', and have not evolved to the self-similar state, then strong vorticity deposition is still possible. We demonstrate this using 2D numerical simulations. The deposition of vorticity and development of density structure depends heavily on the blast waves not having evolved fully to a self-similar state. This hypothetical experiment therefore examines not only the important issues of shock-deposition of vorticity and shock propagation in non-uniform flows, but it also examines the approach of flows towards self-similar states.

Note that throughout this paper we use the term 'blast wave' to refer to strong explosions that are produced by

rapid, localized energy deposition in the most general sense, and not in the more limited sense where the solution has evolved far from its initial conditions. Throughout the paper we discuss the physics using the viewpoint of vorticity deposition and evolution [14], and we work solely in the framework of ideal hydrodynamics. We will also only consider the case of 2D Cartesian geometry in which uniformity is supposed in the ignored coordinate. This means that, prior to interaction, the two blast waves will be cylindrical, axisymmetric blast waves. This minimal problem is particularly relevant to experiments with cluster media where the laser propagates through the cluster medium to produce long 'rods' of strongly heated matter that subsequently produce quasi-cylindrical blast waves. This problem has only indirect relevance to astrophysical problems, since, along with the chosen geometry, precise synchronization of blast waves generation is unlikely in an astrophysical context.

2. Theory

The central idea in this paper is that a binary blast-blast interaction which is asymmetric (in the sense that the explosions are launched from hot spots with somewhat different energy) will experience vorticity deposition (e.g. from inhomogeneous density) when the two blast waves interact and reflected shocks propagate back through the 'cavities' of each blast wave. An illustrative schematic of this interaction is shown in figure 1. The deposition of vorticity can then lead to the generation of complex density structure. The asymmetry is not necessary for vorticity deposition (this also occurs in the symmetric case), but it is relevant to the subsequent development of density structure. Despite the clear combination of shock propagation and density inhomogeneity, the occurrence of strong shock-deposition of vorticity and structure generation is not necessarily obvious.

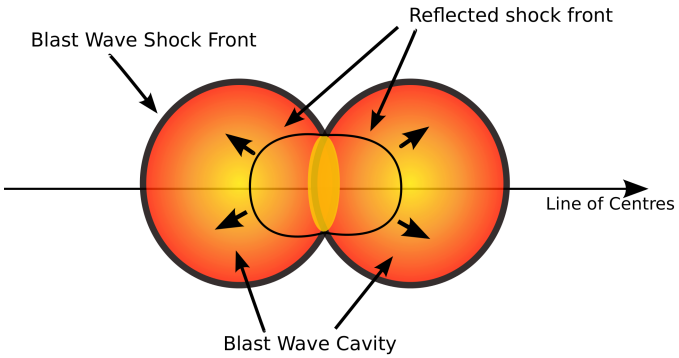

Figure 1: Schematic of binary blast wave interaction.

To explain why, we first consider the shock deposition of vorticity in more detail. The vorticity jump across a shock is a topic with a long history in the scientific literature (see references to Truesdell [15], Lighthill [16], Hayes [17] and Berndt [18]). In relatively recent work, Kevlahan [19] derived an expression for the vorticity jump for the case where the flow is *non-uniform*. Kevlahan's expression is,

$$\delta\omega = \frac{\mu^2}{1+\mu}\frac{\partial C_r}{\partial S} - \frac{\mu}{C_r}\left[\left(\frac{D\mathbf{u}}{Dt}\right)_S + \frac{C_r^2}{1+\mu}\frac{1}{\rho}\frac{\partial \rho}{\partial S}\right] + \mu\omega. \quad (1)$$

In Eq. 1, μ is the density compression factor across the jump, C_r is the shock speed relative to the normal component of the flow ahead of the shock, $\mathbf{u}$ is the velocity vector field of the flow, $\partial/\partial s$ is the tangential part of the directional derivative, and ω denotes the vorticity in the direction $\mathbf{b} = \mathbf{n} \times \mathbf{S}$, where $\mathbf{n}$ is the normal direction to the shock and $\mathbf{S}$ is the aforementioned tangential direction. This equation can be interpreted physically. The first term on the RHS of Eq.1 is the vorticity jump that arises from shock curvature. The second term is baroclinic vorticity generation arising from non-uniformity in the flow. The third term represents conservation of angular momentum.

Since we are considering a system which is initially static, we are therefore automatically dealing with a problem in which the unshocked fluid is vorticity-free. We therefore do not have to consider the third term in the first instance. Prior to interacting we have $\partial C_r/\partial S = 0$ for each blast wave, so if we neglect the possibility that the first term is important (i.e. shock refraction is assumed to be weak), then we are left with the second term. For the case where the un-shocked fluid is isentropic (as it is in the case we consider), the second term can be shown to depend only on $\partial\rho/\partial S$. One can describe a blast wave as consisting of a thin 'shell' surrounding an interior 'cavity' [20]. There exists a well-known self-similar solution by Sedov [21], however the simplified picture will suffice for this discussion. The strongest density gradients are localized to the thin shell, with weaker variation of density inside the cavity. There are therefore two problems with obtaining significant vorticity deposition. On the one hand one might expect the density gradients in the 'cavity' region to be too weak (based on Sedov's solution). On the other hand, although there are strong density gradients in the shell, this region is moving rapidly which means that C_r may not be large. As can be seen in figure 1, once the blast waves interact, the outermost shock front is always moving away from the reflected shock. There is also the issue of shock deceleration on encountering an increasing density gradient which may lead to C_r being small when the reflected shock reaches the shell region. Thus, without detailed calculation, we have good reason to doubt the possibility of significant vorticity deposition.

There is, however, the possibility that if the blast wave has not been able to evolve to the point that it closely matches the Sedov-Taylor state then the density gradients in the cavity may be much stronger than we would anticipate based on Sedov's solution. This would remove the

first obstacle suggested above, and could lead to strong vorticity deposition in the cavity region (although not in the shell). The characteristic time for the blast wave evolution is $\tau = R_h^2\sqrt{\frac{\rho}{\mathcal{E}}}$ [22, 23] (assuming cylindrical geometry; where R_h the characteristic size of the initial hot spots, ρ the ambient density, and $\mathcal{E}$ is the area-integrated energy deposited in the hot spot). When $t \ll \tau$, the explosion cannot have evolved far from its initial conditions. This can be seen by noting that τ is approximately equal to R_h/c_h. On the other hand when $t \gg \tau$ we expect the blast wave to have reached the Sedov phase. Therefore one expects that, for $\tau \approx 1$ that the blast wave will be 'young' in the sense that strong cavitation will have occurred, but that it will still be far from the self-similar state. The blast wave may still be relatively 'young' even up to $\approx 10\tau$. We note that the issue of departure from the self-similar solution has long been noted in astrophysical studies, particularly in the case of supernova remnants [24, 23]. Of course, the density profile of the 'young' blast wave does not have an analytic solution as such, and we must therefore resort to numerical simulations to further investigate this matter.

Finally we note that it is vorticity deposition in the cavity region that is potentially the most interesting possibility. As we are considering asymmetric blast waves, the material that builds up at the intersection of the two blast waves will experience a net drive into the cavity of the weaker blast wave. If there has been copious vorticity deposition then this will strongly influence the evolution of the fluid that flows in. The generation of a jet-like feature may occur along with Kelvin-Helmholtz roll-up.

In summary, when two blast waves interact, reflected shock waves propagate through the internal region bounded by the shock front. Although this region is inhomogeneous, there are good reasons to doubt that there will be significant shock-deposition of vorticity, especially if the blast wave closely resembles the Sedov-Taylor state of evolution. If the blast waves are relatively young then significant vorticity deposition may be possible,but the evaluation of this requires numerical simulation. We now proceed to investigate this possibility through 2D numerical simulations.

3. Numerical Simulations

In order to study vorticity deposition and its consequences, we have carried out two dimensional hydrodynamic simulations using the ARCTURUS code. In the configuration used in this study, ARCTURUS solves the inviscid Euler equations for an ideal gas using the scheme of Ziegler/Kurganov-Noelle-Petrova [25, 26]. We have exploited the fact that the inviscid Euler equations can be cast in dimensionless form by choosing $\tilde{\rho} = \rho/\rho_0$, $\tilde{u} = u/c_0$, $\tilde{P} = P/(\rho_0 c_0^2)$, $\tilde{x} = x/L$, and $\tilde{t} = c_0 t/L$. The parameters ρ_0, c_0, and L are a characteristic density, sound speed and scale-length respectively. Henceforth we will drop use of the tilde and refer only to the dimensionless quantities. The mid-lines of the computational domain shall be denoted by x_m and y_m. As we only deal with the case of an ideal gas we have $\gamma = 5/3$ throughout.

Simulation	d_h	P_{h1}	R_{h1}	P_{h2}	R_{h2}
A	80	40000	10	80000	5
B	80	40000	10	320000	2.5
C	80	40000	10	500000	2
D	80	40000	10	2000000	1

Table 1: Table of simulation parameters.

The initial conditions consist of a uniform, static, ambient medium ($\rho = 1$,$\mathbf{u} = 0$, $P = 1$) that fills nearly the entirety of the domain except for two hot spots. These are two uniform circular regions centred at $x = x_{h1}$ and $x = x_{h2}$ respectively (and $y = y_m$), which will principally be referred to as 'source 1' and 'source 2' respectively, and the use of '1' and '2' in subscripts refers to each source. The hot spots are of the same density as the ambient medium ($\rho = 1$), but substantially higher pressures,P_{h1} and P_{h2} . The fluid is also initially static in the hot spots. The hot spot radii are denoted by R_{h1} and R_{h2}. The pressure profiles used for the hot spots are Gaussians with P_{hi} (where i =1,2) being the peak pressure and R_{hi} being the radius at which the pressure falls to $e^{-1/2}$ of the peak value. The boundary conditions are outflow boundaries in both x and y, although the most important processes (shock deposition of vorticity) occur before the shock front reaches the boundaries. The simulations are run up to at least $t = 4$. The hot spots were always centred symmetrically about $x = x_m$, and we thus just note the hot spot separation (centre-to-centre distance), d_h, when listing parameters, as $x_{h1} = x_m + d_h/2$, and $x_{h2} = x_m - d_h/2$. The simulation parameters for the various runs are tabulated in Table 1 below. Importantly the parameters were chosen so that the total area-integrated energy in the hot spots is kept constant. The two hot spots are chosen to be moderately asymmetric, with the 'hotter' (source 2) one having half the area-integrated energy of the other (i.e. source 1).

With this choice of parameters we have τ =0.024. It was found that the blast waves interact and the reflected shocks cross the cavity in the period t =0.2–0.6, i.e 8τ–25τ. At this point we expect the blast waves to be in a 'marginally young' state.

All simulations were performed on a 2000 × 2000 grid with $\Delta x = \Delta y$ =0.2. This ensure that there are 5 grid points for even the smallest source radius. This means that the total size of the domain in the dimensionless units is 400 × 400, and $x_m = y_m$ =200.

4. Results and Discussion

The main result of these simulations is summarized in figure 2 in which the mass density is plotted for runs A–D at t =3.2, which is some time after the two blast waves have interacted. Only the left side of the simulation domain is shown where the area around source 2 is located.

Simulation	Peak Circulation in Upper Left Quadrant (dimensionless units)
A	-2451
B	-3158
C	-3200
D	-3202

Table 2: Tabulated values of peak circulation in upper left quadrant of simulation box for runs A–D.

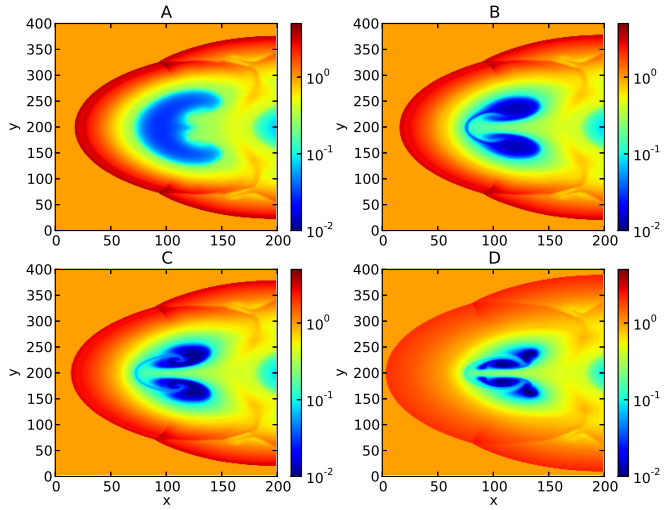

Figure 2: Plots of mass density ($\log_{10}$ scale) at t =3.2 in runs A–D.

Figure 2 shows that the implosion of the cavity of the source 2 blast wave leads to a spike or jet-like protrusion which develops along the line of the centres of the two hot spots. Kelvin-Helmholtz roll-up is also evident along the protrusion and particularly at the mushroom-shaped head of the protrusion. It is also evident that the development of this jet/spike/protrusion is the only significant consequence of shock-deposited vorticity. The shells of the blast waves have clearly continued to propagate outwards without developing any structure. The prediction that structure would only strongly develop in the cavity, and not in the shell, appears to be verified from figure 2. It is clear that the protrusion has developed as a result of vorticity deposition, and that the extent to which it develops depends on the details of the vorticity deposition. In fact in these simulations we observe the formation of a strong vortex pair (which would be a vortex ring in the spherical analogue problem). The comparatively weak development of the protrusion in run A indicates that either there is too little circulation or that the vorticity deposition is geometrically misplaced. When one looks at the peak circulation ($\Gamma = \int \omega . d\mathbf{A}$) in the upper left quadrant of the simulation box, one finds that there are only weak variations between the simulations. This is shown in table 2.

We therefore turn to the suggestion that the location of vorticity deposition is more important. In order to examine this we have plotted the evolution of vorticity at early time, and the evolution of density for runs A and C. Plots of the mass density at early times for run A are shown in figure 3, and for run C in figure 5. Plots of the vorticity at early times in run A are shown in figure 4, and for run C in figure 6. In figures 3–6 only the upper left quadrant of the simulation box is plotted.

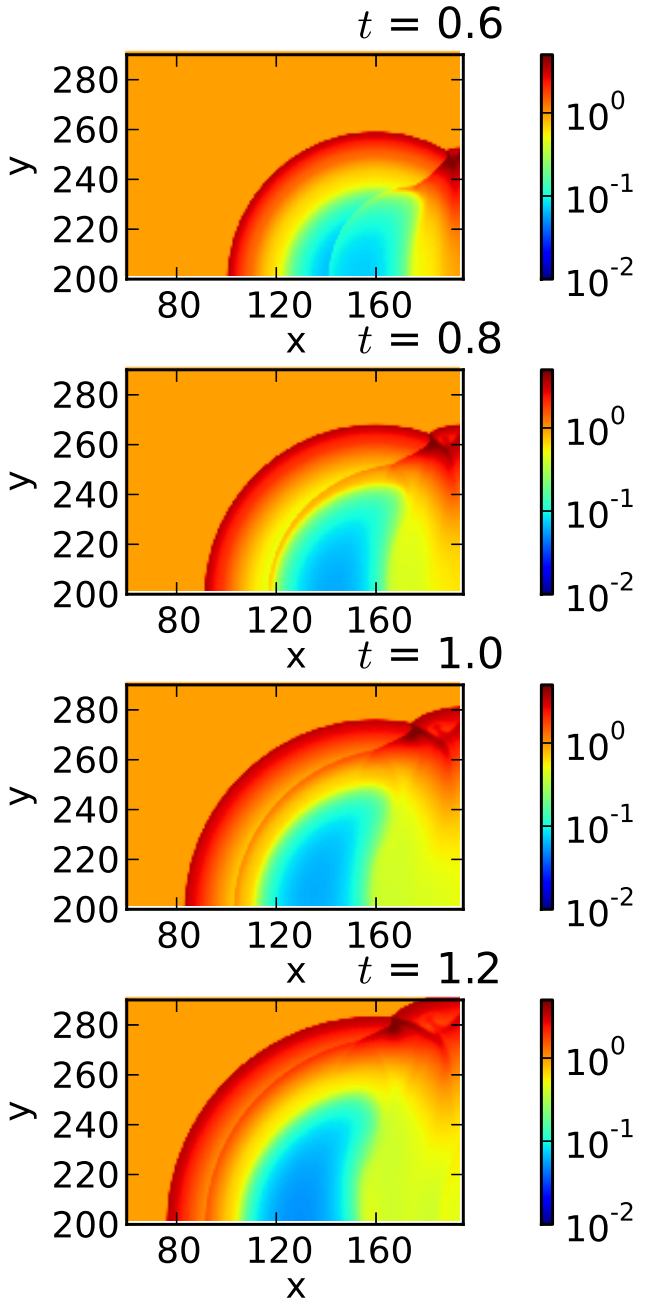

Figure 3: Plots of mass density ($\log_{10}$ scale) at times indicated in run A. Upper left quadrant only (i.e. blast wave around source 2).

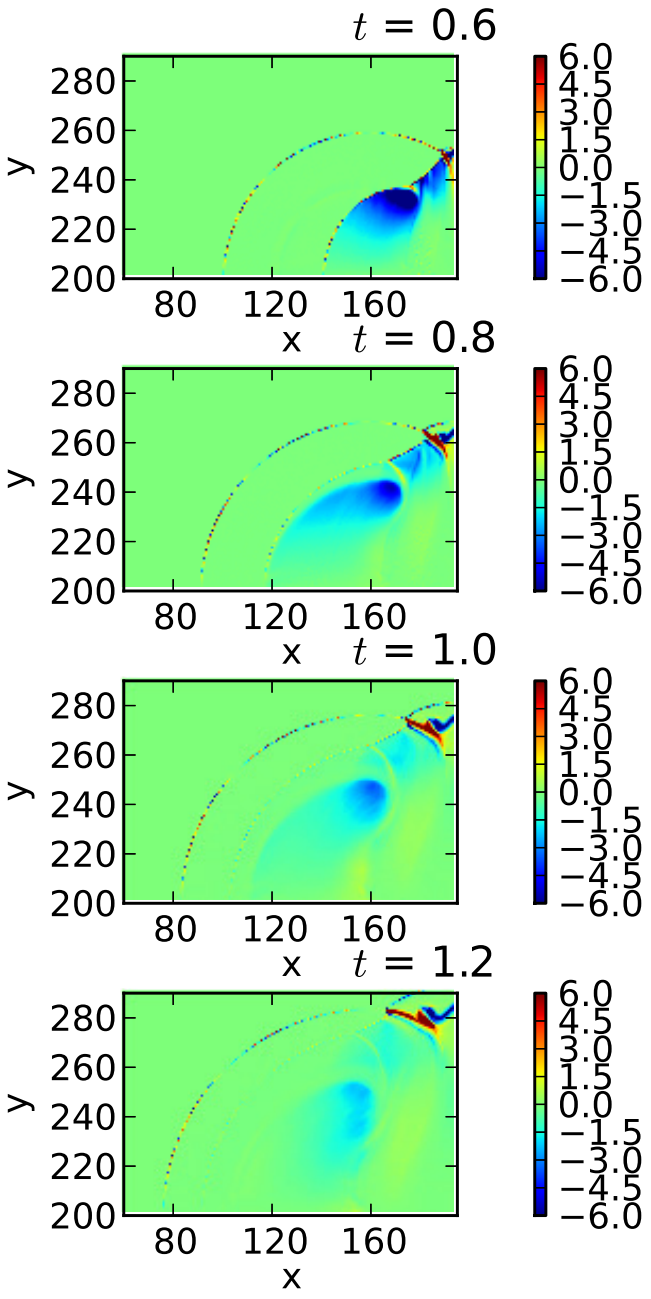

Figure 4: Plots of vorticity at times indicated in run A. Upper left quadrant only (i.e. blast wave around source 2). Note that vorticity of interest is in $x \approx 160, y < 250$ region.

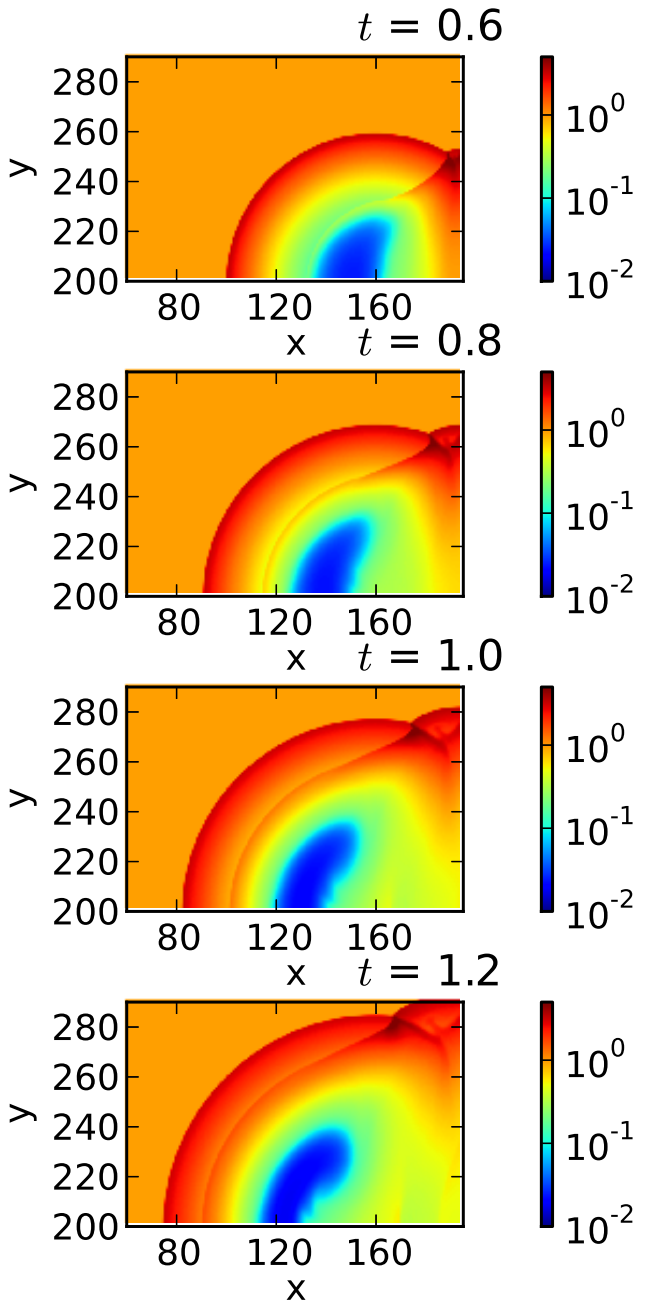

Figure 5: Plots of mass density ($\log_{10}$ scale) at times indicated in run C. Upper left quadrant only (i.e. blast wave around source 2).

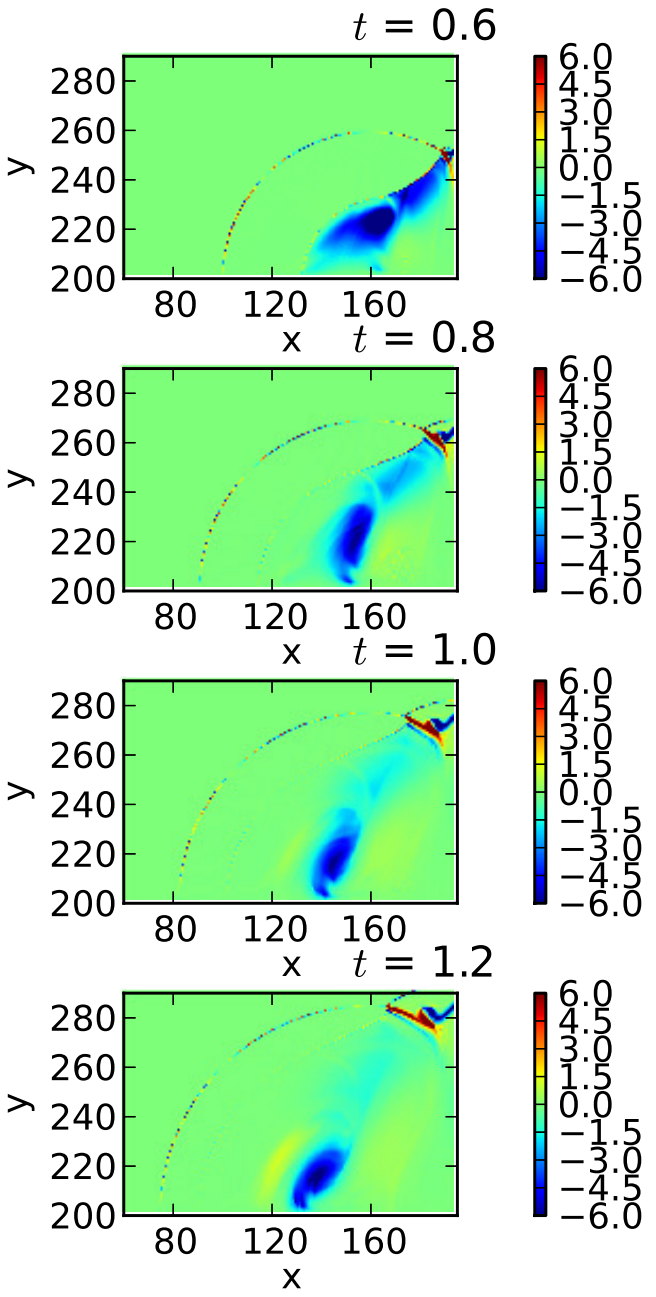

Figure 6: Plots of vorticity at times indicated in run C. Upper left quadrant only (i.e. blast wave around source 2). Note that vorticity of interest is in $x \approx 160, y < 250$ region.

What we observe, particularly by comparing figures 4 and 6, is that, at early times, vorticity is deposited much closer to $y = y_m$ in run C than in run A. The vortex pair will tend to drive the material entering the cavity into a protrusion along the axis of the vortex pair (which coincides with the line of the hot spots), however the width of the protrusion depends on the distribution of vorticity. If the vorticity is weak only along a narrow channel along the axis then the protrusion that grows will be very thin. If the vorticity is weak over a wide region then the protrusion will be wide.

We must also recall the fact that the outward directed velocity grows on moving away from the hot spots. Therefore, vorticity that is deposited away from the hot spot locations will be advectively transported away more strongly than vorticity that is deposited closer to the hot spot locations. By comparing figures 4 and 6 we see that the strongest regions of vorticity at t =0.6 are almost twice as far from the line of hot spots in A than in C. This accounts for the more rapid weakening of vorticity in run A compared to run C, and this is another reason why density structure develops much more slowly in A.

It is therefore apparent that the development of density structure in these simulations is principally being determined by the distribution of vorticity rather than its absolute magnitude or circulation. We now turn our attention to the details of vorticity deposition itself. To examine this we can look at lineouts along y of the mass density runs A and C at t =0.2, which is immediately before the shock crosses the cavity. These lineouts are produced at x =165 which is where strong vorticity deposition occurs.

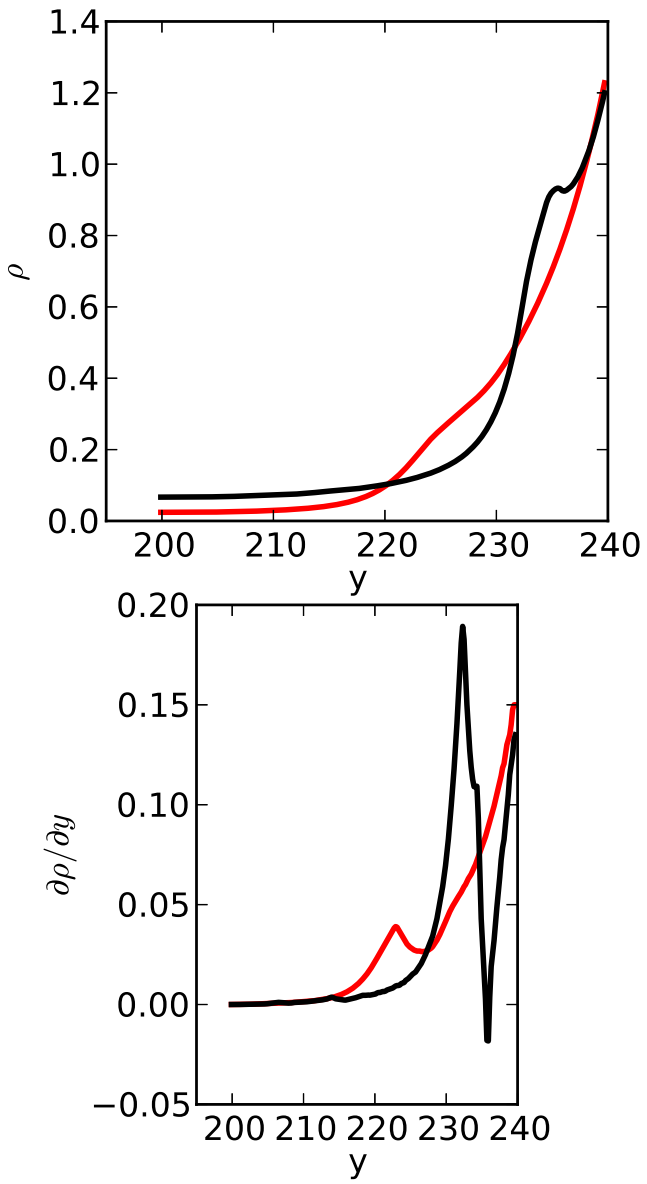

Figure 7: (Upper)Line-out of the mass density in runs A (black) and C (red) at t =0.2 along x =165. (Lower) Line-outs of $\partial\rho/\partial y$ in runs A (black) and C (red) at t =0.2 along x =165.

Figure 7 should be read in comparison with the plots of vorticity (at t =0.4) in figures 4 and 6. In run A we see from figure 4 that peak vorticity deposition occurs around y =230, and from figure 7 we see that this corresponds to where $\partial\rho/\partial y$ rapidly increases. In run C we see from figure 4 that peak vorticity deposition occurs around y =220, and from figure 7 we see that this corresponds to where $\partial\rho/\partial y$ has a local maximum. We also note that $\partial\rho/\partial y$ is much lower around y =220 in run A compared to run C. From this we conclude that the differences in vorticity deposition can be reasonably attributed to the $\partial\rho/\partial S$ term in Eq. 1 alone, and that density inhomogeneities dominate the pattern of vorticity deposition.

Simulation	R^2_{coll}/R^2_{h2}	t_{coll}/τ
A	91.8	21.3
B	367.1	88.2
C	578.4	136.4
D	2371.4	545.5

Table 3: Tabulated values of the 'age' of the blast wave due to source 2 in each simulation according to the mass-swept and dimensional analysis approaches.

It is also apparent from the line-outs shown in figure 7 that it is the non-self-similar nature of the solutions that is critical to the observed behaviour, as anticipated. This conclusion has been reinforced by the results of similar simulations that were initialized with hot spots with 'top-hat' rather than Gaussian pressure profiles in which deviations from the self-similar solution were more obvious. What is curious is that on increasing the weaker hot spots pressure and decreasing its radius we should, from $\tau = R_h^2\sqrt{\frac{\rho}{\mathcal{E}}}$, be increasing its relative 'age' at the time that the blast waves interact. Taking the simulation results at face value, one might believe that the generation of density structure, which becomes more pronounced on going from A to D, is strangely inconsistent with the blast wave from source 2 being 'older' on going from A to D and thus possessing weaker deviations from self-similarity that are required to produce strong vorticity deposition.

The 'age' of the blast wave can also be estimated by the ratio of (area-integrated)mass swept up by the blast wave to the mass in the initial hot spot. In the case of these simulations this simply becomes R^2_{coll}/R^2_{h2}, where R_{coll} is the radius of the shock front at the time of collision. We have calculated both measures of ageing the blast wave from source 2 and we have tabulated the results in Table 3.

As we can see from Table 3 we actually reach the same conclusion using both methods, i.e. the blast wave from source 2 is more developed on going from run A to D. The apparent inconsistency is resolved by returning to figure 7. Looking at this again, we can see that the deviation from smooth self-similar conditions, particularly in terms of $\partial\rho/\partial y$, is much stronger in run A than in run C. However the deviation in run A is located away from the central point of source 2, whereas in run C it is located much closer to the central point of source 2, but the magnitude of $\partial\rho/\partial y$ reached at the local maximum is clearly much less than it is in run A. So on progressing from run A to run D at any chosen time we see that actually the 'older' blast waves have progressed further towards self-similarity and deviations are gradually diminishing. However the geometric location of these deviations is actually more important in this problem, and thus runs C and D produce

more pronounced density structure purely for this reason.

This matter can also be explained by considering the main source of deviation from self-similarity. It is reasonable that a major source of deviation is the point of transition from initially heated material to initially cold material (i.e. the contact discontinuity). This is because there is no process which can remove the entropy discontinuity associated with the contact discontinuity, which implies a long-lived deviation from self-similarity around the contact discontinuity. The location of the contact discontinuity can be estimated by assuming that the initially heated material expands adiabatically and then calculating the radius of the material if its pressure is equal to the core pressure of the Sedov solution (a fixed fraction of the pressure immediately behind the shock front). This yields $R_c \propto R_h^{2/5}$ if the energy of the hot-spot kept constant. This is clearly consistent with the observed shift in the region of highest vorticity deposition closer towards the origin of source 2, and with the observed shift in the deviations from self-similarity towards the origin of source 2. The scaling in the shifts observed in the simulations is in rough agreement with the $\propto R_h^{2/5}$ scaling.

As previously mentioned, the observation of persistent 'transients' has long been noted in astrophysical studies relevant to supernova remnants [24, 23]. It is clear that, at sufficiently early times, the physical solution cannot be identical to the self-similar one and that the physical solution will approach the self-similar one asymptotically [27]. What we have shown in this study is that one can exploit the transient deviations from self-similarity to drastically alter the outcome of a hydrodynamic interaction via shock-deposition of vorticity in a 'hypothetical experiment'. This naturally raises questions about how self-similarity is approached and the precise behaviour of transients. Here we have suggested that the main source of deviation from self-similarity (or at least the most important one in this study) is the contact discontinuity between the initially heated material and the ambient material. Ultimately this question lies outside of the scope of this paper and will have to be addressed in future work.

5. Potential Experimental Regimes

In the preceding section we have worked in dimensionless units, which is useful for theoretical analysis, but is less useful in terms of discussing prospective laser-based experimental regimes. The most important element of the conceptual interaction we have discussed here is the two blast waves interact when the blast waves are 'young'. Since time for the blast waves to collide is on the order of $d/(2c_h)$ (d being the separation of the sources, and c_h is the average of the sound speeds), and the characteristic time for each blast wave is R_h/c_h, the 'age' of the blast waves when they collide can be written as $d/(2R_h)$. This needs to be kept on the order of ≈ 100 or less according to the results obtained in this study. Observations of the system then need to be made up to ten times the time taken for the blast wave to collide. Since this expresses two distances as a ratio, these can be automatically converted into the working units of choice. Experimentally there may be issues in rigorously characterizing R_h in some systems, and this may have to be estimated through numerically modelling interactions. The actual energy scale involved, and the density does not come into this relation. Obviously the conditions for blast wave formation must be satisfied (rapid heating of sources and hot spot pressures much greater than the ambient pressure). Changing the hot spot energy and density of the ambient medium will simply lead to changing the time-scale of the experiment. Therefore this experiment might be realized over a wide range of different configurations including cluster media [10], gas targets [28], and solid targets heated by laser-generated relativistic electrons [29].

6. Conclusions

In this paper we have examined the possibility of vorticity deposition and density structure generation in asymmetric binary blast wave interactions. We have considered a hypothetical experiment consisting of just two blast waves launched from unequal hot spots . When these blast waves interact a reflected shock wave propagates through the interior of the blast wave. As this is inhomogeneous there should be some baroclinic vorticity deposition. However we have argued that for blast waves that have evolved to the Sedov-Taylor state, the vorticity deposition is unlikely to be significant. If, however, the blast waves are at a relatively early phase in their evolution and have not yet reached the fully self-similar state, then strong vorticity deposition remains a possibility, because of the presence of transient deviations from self-similarity which diminish as the blast wave evolves. We have investigated this using 2D numerical simulations. We have found significant vorticity deposition and density structure generation for moderately asymmetric blast waves that interact around 10–20τ (where τ is the characteristic time for blast wave evolution). It would appear that this largely relies upon the blast waves still being somewhat far from the self-similar state at the time they interact. The issue of the approach to self-similarity will be addressed in future work. Given that colliding blast waves has already been achieved [12] in laser interactions with cluster media, it would seem that an experimental investigation of this problem would be a modest extension of previous experimental undertakings (varying energy and possibly focussing of one of the drive beams).

7. Acknowledgements

APLR and HS have carried out this work as part of the European Research Council Starting Grant, STRUCMAGFAST (StG 2012). The authors are grateful for helpful comments made by the anonymous referee.

References

[1] R.E.Pudritz, N.K.-R.Kevlahan, Shock interactions, turbulence and the origin of the stellar mass spectrum, Phil. Transac. of the Royal Soc. A 371 (2013) 20120248.

[2] N.Kevlahan, R.E.Pudritz, Astrophysical Journal 702 (2009) 39–49.

[3] J. R.M.Kulsrud, R.Cen, D.Ryu, The protogalactic origin for cosmic magnetic fields, Astrophysical Journal 480 (1997) 481–491.

[4] H.Xu, et al., The biermann battery in cosmological mhd simulations of population iii star formation, The Astrophysical Journal 688 (2008) L57–L60.

[5] A.R.Miles, The blast-wave-driven instability as a vehicle for understanding supernova explosion structure, Astrophysical Journal 696 (2009) 498–514.

[6] K.Matsuura, et al., Science 333 (2011) 1258–1261.

[7] T.Ma, et al., Onset of hydrodynamic mix in high-velocity, hihigh compressed inertial confinement fusion implosions, Phys.Rev. Lett. 111 (2013) 085004.

[8] A.D.Edens, et al., Study of high mach number laser driven blast waves, Phys. Plasmas 11 (2004) 4968.

[9] G.Gregori, et al., Generation of scaled protogalactic seed magnetic fields in laser-pro shock waves, Nature 481 (2012) 480–483.

[10] D.R.Symes, et al., Investigations of laser-driven radiative blast waves in clustered gases, High Energy Density Phys. 6 (2010) 274–279.

[11] R. A. T.Handy, T.Plewa, Prospects of turbulence studies in high-energy density laser-generated plasma: Numerical investigations in two dimensions, High Energy Density Phys. 11 (2014) 1–11.

[12] R.A.Smith, et al., High resolution imaging of colliding blast waves in cluster media, Plasma Phys. Control. Fusion 49 (2007) B117–B124.

[13] D.Ranjan, J.Oakley, R.Bonazza, Shock-bubble interactions, Annu.Rev.Fluid Mech. 43 (2011) 117–140.

[14] J.F.Hawley, N.J.Zabusky, Vortex paradigm for shock-accelerated density-stratified interfaces, Phys.Rev.Lett. 63 (1989) 1241–1244.

[15] C.Truesdell, J.Aero.Sci. 19 (1952) 826–828.

[16] M.J.Lighthill, J.Fl 2 (1957) 1–32.

[17] W.D.Hayes, J.Fluid 2 (1957) 595–600.

[18] S.B.Berndt, J.Fluid M 26 (1966) 433–436.

[19] N.K.-R.Kevlahan, The vorticity jump across a shock in a non-uniform flow, J.Fluid Mech. 341 (1997) 371–384.

[20] Ya.B.Zel'dovich, Yu.P.Raizer, Physics of Shock Waves and High-Temperature Hydrodynamic Phenomena, Dover, 2002.

[21] L.I.Sedov, Similarity and Dimensional Methods in Mechanics, Academic Press (New York), 1959.

[22] T.E.Fox, et al., Phys.Plasmas 21 (2014) 102110.

[23] S.F.Gull, MNRAS 171 (1975) 263.

[24] D.F.Cioffi, C.F.McKee, E.Bertschinger, Astrophys.J. 334 (1988) 252.

[25] U.Ziegler, A central-constrained transport scheme for ideal magnetohydrodynamics, J.Comput.Phys. 196 (2004) 393–416.

[26] A.Kurganov, S.Noelle, G.Petrova, Semidiscrete central-upwind schemes for hyperbolic conservation laws and hamilton-jacobi equations, SIAM J.Sci.Comput. 23 (2001) 707–740.

[27] G.I.Barenblatt, Ya.B.Zel'dovich, Self-similar solutions as intermediate asymptotics, Annu.Rev.Fluid Mechanics 4 (1972) 285–312.

[28] J.M.Picone, J.P.Boris, Vorticity generation by asymmetric energy deposition in a gaseous medium, Phys. Fluids 26 (1983) 365–382.

[29] A.P.L.Robinson, H.Schmitz, J.Pasley, Phys.Plasmas 20 (2013) 122701.